Unimolecular HCl Elimination from 1,2-Dichloroethane: A Single Pulse Shock Tube and ab Initio Study†

B. Rajakumar,‡ K. P. J. Reddy,§ and E. Arunan*,‡

Department of Inorganic and Physical Chemistry and Department of Aerospace Engineering, Indian Institute of Science, Bangalore, India 560012

Received: January 8, 2002; In Final Form: March 25, 2002

Thermal decomposition of 1,2-dichloroethane (1,2-DCE) has been studied in the temperature range of 1050−1175 K behind reflected shock waves in a single pulse shock tube. The unimolecular elimination of HCl is found to be the major channel through which 1,2-DCE decomposes under these conditions. The rate constant for the unimolecular elimination of HCl from 1,2-dichloroethane is found to be $10^{13.98\pm0.80}$ exp(−57.8 ± 2.0/*RT*) s^{-1}, where the activation energy is given in kcal mol^{-1} and is very close to that value for CH_3CH_2Cl (EC). Ab initio (HF and MP2) and DFT calculations have been carried out to find the activation barrier and the structure of the transition state for this reaction channel from both EC and 1,2-DCE. The preexponential factors calculated at various levels of theory (HF/6-311++G**, MP2/6-311++G**, and B3LYP/6-311++G**) are ($\approx 10^{15}$ s^{-1}) significantly larger than the experimental results. If the torsional mode in the ground state is treated as free internal rotation the preexponential factors reduce significantly, giving excellent agreement with experimental values. The DFT results are in excellent (fortuitous?) agreement with the experimental value for activation energy for 1,2-DCE while the MP2 and HF results seem to overestimate the barrier. However, DFT results for EC is 4.5 kcal mol^{-1} less than the previously reported experimental values. At all levels, theory predicts an increase in HCl elimination barrier on β-Cl substitution on EC.

I. Introduction

The decomposition of 1,2-dichloroethane (1,2-DCE) has received enormous attention over the last five decades. The literature on this reaction can be arbitrarily divided into fundamental[1−9] and applied[10−12] studies. All the "applied" studies concern themselves with improving the production of the vinyl chloride, which is the raw material for the manufacture of the industrially important poly(vinyl chloride), PVC. The fundamental studies, naturally, concern themselves with the rate and mechanism of this process. The general conclusion from thermal studies in static cells[1−4] is that the 1,2-DCE decomposition primarily occurs through C−Cl bond dissociation. On the other hand chemical activation studies[5−7] conclude that the HCl elimination is more important for 1,2-DCE with 90 kcal mol^{-1} internal energy. Continuous wave CO_2 IR laser[8] and KrF UV laser[9] induced thermal decomposition studies, also in static cells, support the C−Cl bond dissociation pathway. Single pulse shock tube is ideally suited for thermal decomposition studies unaffected by surface effects.[13] However, so far such a study has not been attempted to the best of our knowledge.

The 4-center HX elimination reactions from various haloethanes have likewise been studied, both experimentally[14−21] and theoretically,[22−25] for a long time. The nature of the transition state for elimination reactions,[25] the substituent effect on the HX elimination barrier,[17,26,27] and the energy disposal to HX[17] have all been discussed in detail. The nature of the transition state (TS) has particularly been actively debated,[25] with theoretical results mostly favoring a "loose" TS compared to what is predicted from experimental preexponential factors.

Tsang reported the first study on the decomposition of EC using a single pulse shock tube[19] with a rate constant for HCl elimination as 1.44×10^{13} exp(−56.5/*RT*) s^{-1}. (The activation energy and barriers are given in kcal mol^{-1} here and throughout the paper). Setser and co-workers assumed that the HCl elimination barrier from 1,2-DCE would be equal to that of EC, but cautioned that it may be a lower limit.[5] In fact, Dees and Setser[6] later on suggested that the HCl elimination barrier for 1,2-DCE should be higher than that of EC. However, several groups[7,28] have used this assumed value in their work as no experimental value is available yet. The fact that no experimental value is available for this reaction has led to a more serious consequence as well. Chuchani et al. reported a comprehensive study of the β-substitution effect on the kinetics of substituted ethyl chloride pyrolysis in the gas phase.[27] For 1,2-DCE, they have taken the rate constant from Barton's work[1] which proved that the pyrolysis was dominated by C−Cl dissociation. A casual look at Table 3 in ref 27 immediately reveals that the 1,2-DCE data does not fit in well with the data from the other 15 β-substituted ethyl halides. Still, the Taft plot given[27] shows very good agreement for 1,2-DCE, most likely due to the fact that both A and E_a are small.

What would be the effect of β-Cl substitution in EC, on the HCl elimination barrier? The β-F substitution in EC raises the activation energy for HCl elimination[21] by 5 kcal mol^{-1}. Ab initio calculations at the MP2/6-31G* level, qualitatively supported by infrared chemiluminescence experiments, predict that the β-F substitution in CH_3COCl increases the barrier for HCl elimination[17] by 12 kcal mol^{-1}. Holmes and co-workers[26] have shown that the α-substitution by F/Cl increases the barrier for HF elimination but decreases the barrier for HCl elimination from haloethanes. However, both F and Cl when substituted at the β-carbon increase the barrier for dehydrohalogenation. Is it

† Part of the special issue "Donald Setser Festschrift".
* Corresponding author.
‡ Department of Inorganic and Physical Chemistry.
§ Department of Aerospace Engineering.

10.1021/jp020008q CCC: $22.00
Published on Web 05/11/2002

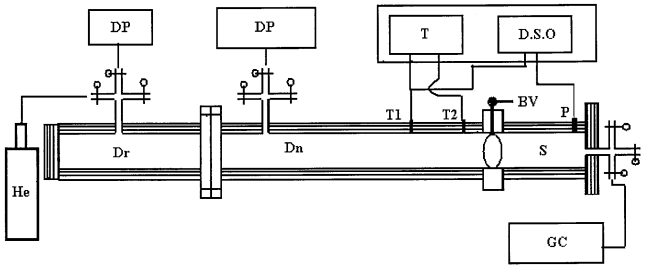

Figure 1. Schematic diagram of the shock tube: DP − 6-in. diffusion pump; Dr − driver section; DSO − digital storage oscilloscope Tektronix, TDS 210; Dn − driven section; S − sample chamber; T1 and T2 − homemade thermal sensors; T − HP 5314A counter; P − pressure transducer, Kistler model 601 A; BV − ball valve; GC − HP 6890^{plus} Gas Chromatograph with FID detector.

likely that the HCl elimination barrier in 1,2-DCE is significantly higher than that of EC, resulting in preferential C−Cl dissociation as observed in all static cell experiments? Or, is it the wall effects in the static cell experiments that make the higher barrier C−Cl dissociation (81 kcal mol^{-1})[29] the dominant channel? Surprisingly, to the best of our knowledge, there is no theoretical estimate on the HCl elimination barrier for 1,2-DCE as well. The ab initio CI study on DCE pyrolysis by Cardy et al.[30] considers C−Cl dissociation only, naturally influenced by the thermal studies so far. On the other hand, the comprehensive theoretical study of HX elimination from haloethanes by Kirtman and co-workers[25] considered only the α-substitution effect on the barrier. Weissman and Benson[31] have reported estimates for the activation energy for EC and 1,2-DCE as 56.4 and 58 kcal mol^{-1}, respectively, predicting a modest increase in HCl elimination barrier on β-Cl substitution.

This paper reports our results from both experimental (single pulse shock tube) and theoretical (ab initio and DFT calculations) studies on the thermal decomposition of 1,2-DCE. Theoretical calculations have been carried out on EC as well to address the β-substitution effect. Shock tube studies have been carried out at the Indian Institute of Science over the last three decades, mainly addressing problems in aerodynamics.[32,33] Recently, a chemical shock tube laboratory has been established, the details of which are given below.

II. Experimental Details

The shock tube used in this investigation is an aluminum tube of 51 mm internal diameter and 25 mm wall thickness. The schematic diagram of the shock tube is shown in Figure 1. The ratio of the driven section length to driver section length is fixed to approximately 2 and their lengths are 2581 and 1276 mm, respectively. The lengths of both the driven and the driver sections can be adjusted by adding or removing small segments of the tube. A pressure transducer (Kistler model: 601A) is mounted at 25 mm from the end flange to record the pressure trace from the primary and the reflected waves. Historically, single pulse shock tube studies have benefited from two attachments to the shock tube i.e., a dump tank in the driven section near the diaphragm and ball valve(s) at the end.[34,13] The effect of the dump tank has never been fully understood and today some laboratories[35] do not use dump tanks in the shock tube. The ball valve is essential for fixing the dwell time.[36] In designing our shock tube, an RCM package[37] was used to simulate the shock waves for our conditions. The length of the shocked region between the contact surface and the primary shock front was determined at every point in the shock tube from the simulations. The lengths of the driver and driven sections were chosen such that the expansion fan cools the heated sample before the reflected wave meets the contact surface. The location of the ball valve (300 mm from the end flange) was chosen to ensure that the compressed test gas occupied a region around the pressure transducer. Hence, the dwell time measured from the pressure trace is very close to the reaction time, i.e., the time for which the molecules were kept at the temperature behind the reflected wave, T_5. The pressure trace given in Figure 2 clearly shows the well-defined dwell time and the arrival of the expansion fan resulting in rapid quenching of the test gas. The inner surface of the ball valve is in flush with the inner walls of the shock tube. Two homemade platinum thin film thermal sensors, mounted at 304 mm apart toward the end portion of driven section, are used to monitor the shock velocity. The outputs from the two sensors trigger a counter (HP 5314A) to start and stop counting. The output from one of the sensors is also used as the trigger for the digital oscilloscope (Tektronix, TDS 210) which collects the pressure signal from the transducer. Thus, the shock velocity could be independently measured using the scope and cross-checked with that measured from the timer. An aluminum diaphragm separates the driver and driven sections. Helium is used as the driver gas.

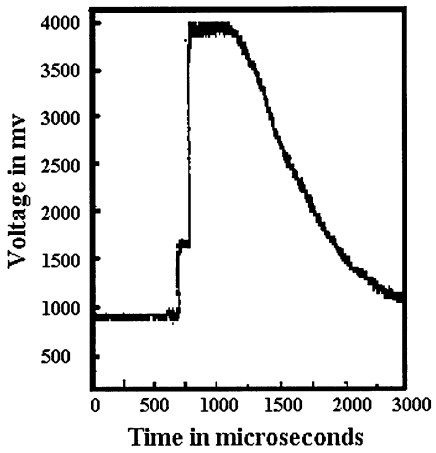

Figure 2. A typical pressure trace recorded by the oscilloscope showing the arrival of primary and reflected shock waves and the expansion wave. The dwell time is measured using such traces. In addition, the time between trigger and the primary/reflected shock wave also gives a measure of shock velocity.

The experimental procedure is very similar to that suggested by Tsang for single pulse shock tube experiments.[19] A 6-in. diffusion pump is used to evacuate the shock tube to $<10^{-5}$ Torr before the experiments. A 1% mixture of 1,2-dichloroethane in argon (which is premixed in a 10 L Pyrex glass bulb) is loaded into the sample chamber (S in Figure 1) to 20 Torr pressure using a mercury manometer, after closing the ball valve. This sample is further diluted with argon until a desired pressure is reached. In all our experiments, this pressure (P_1) was varied between 450 and 600 Torr. The pressure P_5, behind the reflected wave as calculated using ideal shock relations, was between 10 and 15 atm in all runs. If P_1 is kept below 300 Torr, under our conditions the reflected wave meets the contact surface before the arrival of the expansion fan resulting in multiple reflection at the interface that was clearly evident from the pressure trace. The driven section between the ball valve and the diaphragm was filled only with argon to a slightly larger pressure (2−4 Torr higher) than the sample chamber to avoid back diffusion of the test gas. The reactant 1,2-dichloroethane, which is supplied by SD Fine chemicals, India (99.98% stated purity), was triple distilled. In addition, for degassing and further purification, a freeze−pump−thaw method was used several

TABLE 1: The Temperature Behind Reflected Shockwave (T_5) Determined Using Three Different Methods

no.	T_5 (M_s)[a]	T_5 (M_r)[b]	T_5 (kinetic)[c]
1	1068	1000	991
2	1094	1035	1024
3	1146	1056	1031
4	1153	1087	1060
5	1157	1082	1061
6	1236	1138	1104
7	1236	1138	1107
8	1261	1172	1125
9	1325	1232	1171
10	1384	1278	1210

[a] Calculated from the measured incident shock velocity and ideal shock relations. [b] Calculated from the measured incident and reflected shock velocity without any assumptions about the particle velocity in the reflected zone. See ref 36 for details. [c] Determined using the kinetic parameters for $CH_3CH_2Cl \rightarrow C_2H_4 + HCl$ reaction from ref 38.

times before making the sample. The purity of the reactant was frequently tested by gas chromatography.

The temperature behind the reflected wave, T_5, was calculated using the best two of the four methods discussed in detail in ref 36. The first method is the most commonly employed method, in which all the shock properties are calculated from measured incident shock velocity using normal shock relationships. The second method is based on measured incident and reflected shock velocities without any assumption on the particle velocity behind the reflected shock. In addition, the reflected temperature was determined with a chemical thermometer used as an external standard. We have chosen to use the thermal decomposition of EC as the standard reaction, as both (expected) activation energy and enthalpy of reaction are comparable to that of 1,2-DCE. This reaction has been studied in the shock tube by Tsang[19] and by Tschuikow-Roux and co-workers.[38] Tsang's study covered the temperature range 820−1000 K and he reported the rate constant to be $10^{13.2\pm0.1}$ exp(−56.5 ± 0.5/*RT*) s^{-1}. Tschuikow-Roux's work covered the temperature range 960−1100 K and the rate constant was reported as $10^{13.8\pm0.2}$ exp(−57.8 ± 1.0/*RT*) s^{-1}. The latter work covers the temperature range closer to our work. Moreover, it has been pointed out earlier that the preexponential factor reported by Tsang might be low.[5,6] We have used the rate constant reported by Tschuikow-Roux as the standard in our work. Instead of using it as an internal standard, experiments were carried out independently as the products from both reactions could be the same. If C−Cl dissociation should happen from 1,2-DCE, ethylene could be a product from secondary dissociation of the CH_2CH_2Cl radical.[11,12] The T_5 values calculated using these three different methods are given in Table 1. Our results from the various methods are comparable to that reported by Tschuikow-Roux.[36] In kinetic analysis with 1,2-DCE data, the external standard temperature was used. After this work was completed, we came across a paper by Brezinsky and co-workers,[39] which discusses the calibration of the shock tube externally using several chemical reactions.

The post shock gas mixture was analyzed quantitatively by GC (HP 6890^{plus} with flame ionization detector) and qualitatively by IR (Bruker Equinox 55 FTIR). Samples were analyzed in GC by injecting 0.5 mL of the mixture through an online sampling valve. Porapak "Q" packed column was found to be suitable for the reactant and products, viz., 1,2-dichloroethane, vinyl chloride, acetylene, ethyl chloride, and ethylene. Nitrogen (99.999% pure) has been used as the carrier gas at a constant flow rate. The GC analysis was carried out at a constant oven temperature. The GC was calibrated with standard samples: 1,2-DCE (SD Fine Chemicals, India), ethyl chloride and vinyl chloride (Fluka), ethylene (Hydrogas), and acetylene. Acetylene and the other gases used in GC analysis such as argon, helium, oxygen, and hydrogen were from Bhoruka Gases, India (UHP grade 99.999).

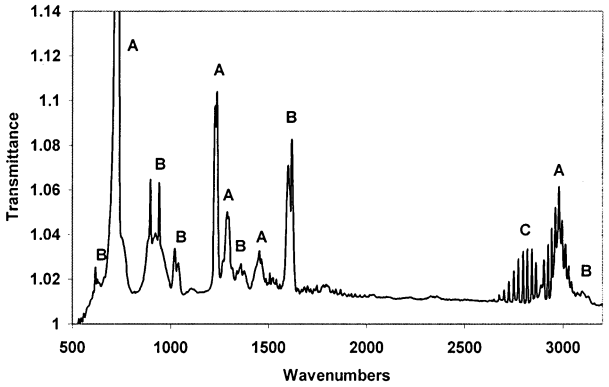

Figure 3. Infrared spectrum of the post-shocked mixture heated to 1150 K. All the peaks are assigned to (A) 1,2-DCE, (B) vinyl chloride, and (C) HCl.

III. Computational Details

All Calculations have been performed with the GAUSSIAN-94 program suite.[40] Geometry optimizations have been carried out at HF, MP2(FULL), and DFT levels with the standard 6-31G*, 6-31G**, and 6-311++G** basis sets internally available in the program suite. Equilibrium and transition state structures were fully optimized at the Hartee-Fock, second-order Møller−Plesset perturbation theory with all the electrons correlated, and density functional theory using B3LYP correlation functional. All the transition states have been characterized with frequency analysis. Zero-point energies and thermal corrections have not been scaled. These results were used in performing transition state theory (TST) calculations to predict the activation energy and the preexponential factors for the HCl elimination reactions for comparison with experimental measurements.

IV. Experimental Results

The IR spectrum of the post-shocked sample obtained from an experiment with 1,2-DCE carried out at 1140 K is shown in Figure 3. It reveals the presence of 1,2-DCE, vinyl chloride, and HCl only. The product composition was independently confirmed by GC analysis, though HCl was not followed by GC. The complete data are given in Table 2. It includes the temperature T_5 determined by using the external standard method, P_5 calculated using the standard shock relations, concentrations of 1,2-DCE and vinyl chloride, and the dwell time for 17 experiments in the temperature range 1050−1175 K. The major products are only vinyl chloride and HCl in the temperature range of 1050−1150 K. Small amounts of acetylene could be observed in the runs above 1160 K. Acetylene formation is through the well-known[41] unimolecular elimination of HCl from vinyl chloride:

$$C_2H_3Cl \rightarrow C_2H_2 + HCl \qquad (R1)$$

The sum of all the concentrations in the post-shocked mixture was used as the initial concentration of the reactant following the established procedures.[13] However, the mass balance was always checked and the initial concentration of 1,2-DCE was

TABLE 2: Summary of the Experimental Results for 1,2-DCE

no.	P_5 (atm)	T_5 (K)	dwell time (μs)	$[DCE]_t/[DCE]_0$	$[VC]_t/[DCE]_0$	k (s^{-1})
1	13.2	1071	520	0.935	0.065	128
2	13.4	1083	528	0.857	0.143	290
3	12.9	1088	516	0.882	0.118	242
4	11.2	1088	520	0.882	0.118	245
5	12.6	1099	504	0.873	0.127	275
6	14.7	1100	516	0.832	0.168	376
7	10.0	1103	512	0.858	0.142	300
8	10.5	1113	520	0.811	0.189	402
9	14.1	1113	512	0.845	0.155	327
10	14.3	1114	548	0.678	0.322	710
11	11.5	1115	528	0.809	0.191	420
12	14.3	1116	592	0.738	0.262	533
13	14.1	1127	572	0.723	0.277	568
14	15.0	1136	588	0.680	0.320	655
15	11.7	1144	568	0.567	0.408	1000
16	14.2	1153	720	0.367	0.577	1391
17	13.5	1174	604	0.424	0.488	1422

always within 10% of the sum of reactant and products. The trends of the reactant 1,2-DCE and the product vinyl chloride are shown in Figure 4. The deviation of concentration of vinyl chloride after 1160 K in Figure 4 is due to the conversion of vinyl chloride to acetylene. From the [1,2-DCE] before and after the experiments, the first-order rate constant for the disappearance of [1,2-DCE] was determined at various temperatures. The Arrhenius plot of the experimental rate constants is shown in Figure 5. From this plot, the preexponential factor and activation energy are found to be $10^{13.98\pm0.80}$ s^{-1} and 57.8 ± 2.0 kcal mol^{-1}, respectively. These values (especially A) are very similar to that obtained for unimolecular elimination reactions.[13] These parameters would fit very well with the 15 other β-substituted ethyl chlorides in Table 3 of ref 27. Though, C−Cl dissociation of 1,2-DCE also results in the formation of vinyl chloride through a chain mechanism, the kinetic parameters are very different. Moreover, there was no evidence for ethylene within the temperature range studied. Tshuikow-Roux[20] and co-workers have identified C−Cl bond dissociation pathways from CF_3CH_2Cl at temperatures above 1300 K, by identifying other products. We conclude that the 1,2-DCE pyrolysis in the temperature range 1050−1175 K is dominated by unimolecular HCl elimination only:

$$CH_2Cl{-}CH_2Cl \rightarrow CH_2{=}CHCl + HCl \qquad (R2)$$

It should be noted that Hassler and Setser[5] considered falloff effects in the HCl elimination reactions for these two molecules and 1,1-DCE. They concluded that at $P = 10^3$ Torr (1.3 atm), these reactions are at the high-pressure limit. Our experimental pressure was 10−15 atm, and there was no evidence to suggest otherwise. Karra and Senkan[42] have also analyzed the falloff behavior for these reactions and they predicted falloff effects up to $P = 10$ atm and $T = 500-1700$ K, very close to our experimental conditions. However, our experimental rate constant is in close agreement with their high-pressure limit. Moreover, Karra and Senkan[42] clearly pointed out the lack of experimental data on this reaction and cautioned that their results await experimental verification.

The Cl atom substitution at the β-carbon of EC does not increase the activation energy for HCl elimination significantly, validating the estimate of Benson[31] and the assumption of Hassler and Setser.[5] Later, Dees and Setser[6] had favored a 4−5 kcal mol^{-1} increase in barrier for 1,2-DCE compared to EC to explain the difference in $k(E)$ between EC and 1,2-DCE. Our

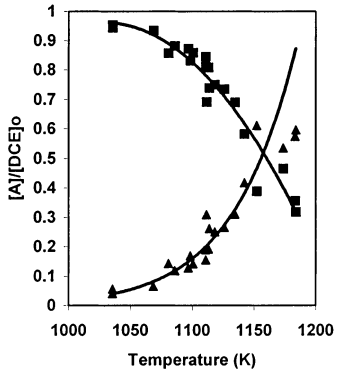

Figure 4. The concentration profile of 1,2-DCE and vinyl chloride as a function of T. [A] = 1,2-DCE solid squares and [A] = vinyl chloride solid triangles.

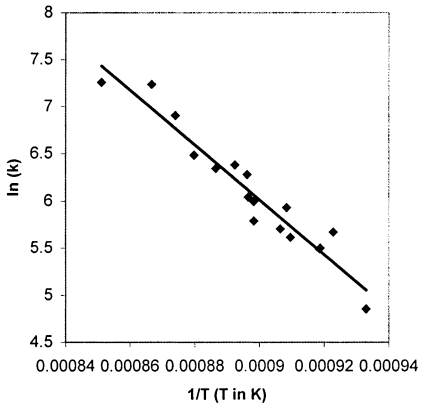

Figure 5. Arrhenius plot for the decomposition of 1,2-DCE.

experiments do not indicate a significant difference in activation energy between the two molecules. Theoretical calculations, including electron correlation, do predict a modest increase in the barrier (3−4 kcal mol^{-1}) and they are discussed next.

V. Computational Results and Discussion

Our main objective in the computational work was to identify the TS for HCl elimination and estimate the preexponential factor and activation energy for the reaction. Hence, both ground state and TS structures were fully optimized at HF, MP2, and DFT (B3LYP) levels with the standard 6-31G*, 6-31G**, and 6-311++G** basis sets. To verify the β-substitution effect of Cl, calculations were carried out for EC and trans and gauche forms of 1,2-DCE. Tables IS, IIS, and IIIS give the optimized structures of EC, trans and gauche 1,2-DCE reactants at various levels of calculations. (Table numbers XS are to be found in Supporting Information). There have been several reports on the equilibrium structure of these two reactants.[43,44] We just note that our results are in complete agreement with earlier reports at the same level of calculations. For 1,2-DCE, the C−Cl distance in the trans form is 0.01 to 0.03 Å longer than in the gauche form at various level of calculations. This influences the low-frequency normal mode vibrations (CCCl deformation and CCl stretching) for the two conformers and the TST rate constants, vide infra. Extensive searches were made for the transition state structure for HCl elimination reactions as it was felt that most of the earlier work[17,25,45] found too long a C−Cl distance for the TS. The C−Cl distance was varied from that of the reactant itself. However, TS optimization for both these molecules always resulted in similar long C−Cl distances. Tables IVS and VS give the optimized structures for the TS

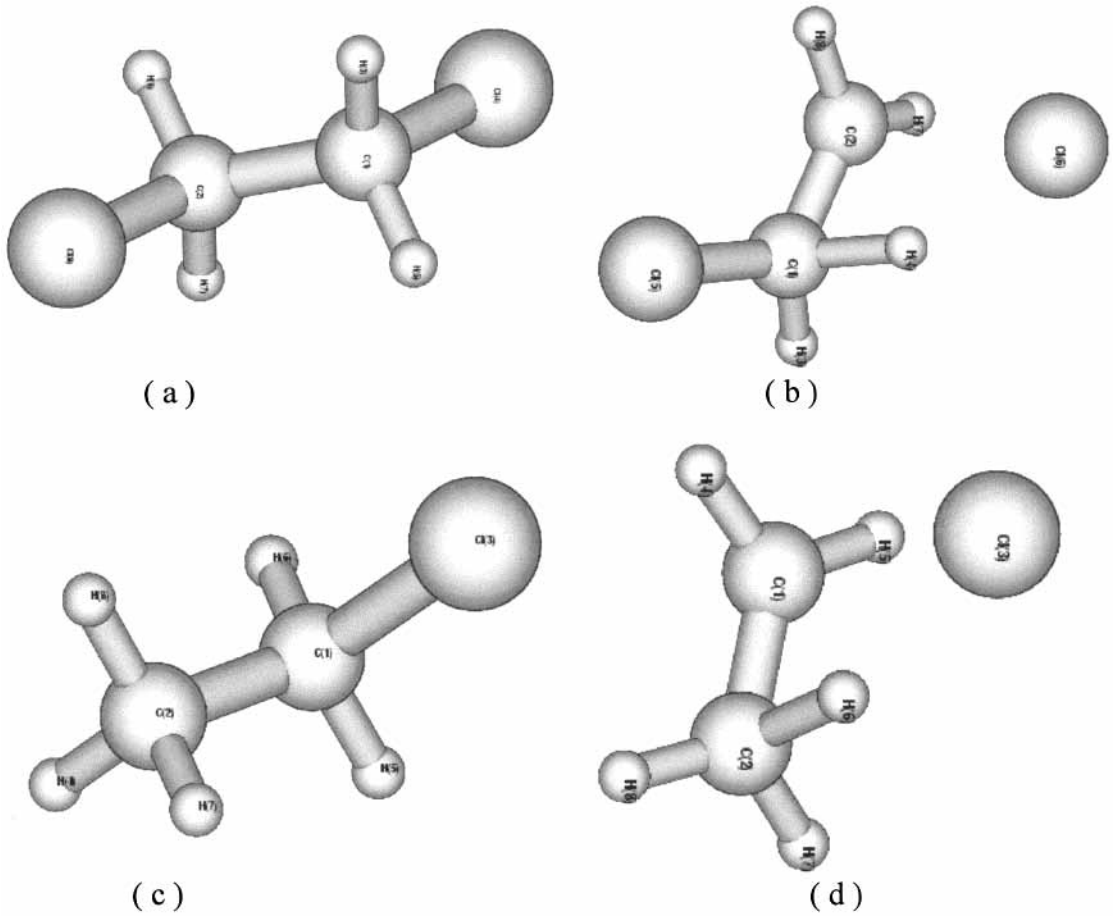

Figure 6. Optimized structures of (a) *trans*-1,2-DCE; (b) TS for HCl elimination from 1,2-DCE; (c) EC and (d) TS for HCl elimination from EC. Detailed structural parameters (including for *gauche*-1,2-DCE) calculated at HF, MP2, and DFT level calculations with 6-31G*, 6-31G**, and 6-31++G** basis sets are given in Tables IS−VS in Supporting Information.

for HCl elimination from both reactants. Only for EC, theoretical results at HF/6-31G** are available,[25] and they are in complete agreement with our results at the same level.

The structure of the ground and the transition states are shown in Figure 6. The TS has a plane of symmetry for EC, containing all the four atoms involved in the reaction, i.e., two carbon, hydrogen, and chlorine. The ∠ClCCH dihedral angle is 0° at all levels of theory. For 1,2-DCE, the four atoms were almost in a plane and the dihedral angle varied between −0.7 to −3.0° at various levels. At the HF level, the C−C bond distance in 1,2-DCE at the TS is 1.379 Å with 6-31G** basis and adding the diffuse functions (6-311++G**) increases it to 1.390 Å. Adding electron correlation results in further increase and both at MP2/6-311++G** and B3LYP/6-311++G** levels, the C−C distance is 1.397 Å. This C−C distance corresponds to a bond order of about 1.5, very close to that of benzene. On the other hand, the C−Cl distance at the TS decreases with basis set size going down from 2.687 to 2.511 Å between HF/6-31G** and HF/6-311++G**. Adding electron correlation at the MP2 level decreases the C−Cl distance to 2.415 Å, but the DFT calculation shows an increase to 2.599 Å. The C−Cl distance is directly related to the "looseness" of the TS and it is clear that DFT predicts a looser TS than MP2 as observed in our earlier work on HNFCl.[45] It should be noted, however, that even for the ground state, the C−Cl distances change in a similar fashion at the three levels of theory for EC and 1,2-DCE. The breaking C−H bond distances were similar for the two molecules and it increased by 0.04 Å from HF level (1.23 Å) to MP2 and DFT levels (1.27 Å).

Frequency calculations were carried out at most of these levels both for the ground and transition states. Tables VIS−XS list the frequencies at various levels for EC, trans- and gauche-1,2-DCE, and TS for HCl elimination from the two reactants. The longer C−Cl distance in the *trans*-1,2-DCE results in significantly lower C−Cl stretching and CCCl deformation frequencies in the trans compared to the gauche form. MP2 calculations give two CCCl deformation frequencies as 223 and 315 cm^{-1} for trans and 271 and 426 cm^{-1} for gauche. The corresponding experimental values are 222, 300, 272, and 410 cm^{-1}, respectively.[46] The torsional frequency is the same in both forms. The TS were characterized by one imaginary frequency corresponding to the reaction coordinate. At the TS, the C−Cl bond is nearly broken and the C−H bond is partially broken. The motion of the reaction coordinate when visualized with Molden[47] confirmed that the TS corresponded to the reaction of interest. At all levels of theory, the motion of the reaction coordinate was dominated by H atom moving away from C and joining Cl.

The thermal rate constants for the HCl elimination from C_2H_5Cl and 1,2-DCE were calculated using the transition state theory expression for rate constant:[48]

$$k(T) = l\frac{k_B T}{h}\frac{Q_{\ddagger}}{Q_R}\exp\left[-\frac{E_0}{RT}\right] \qquad (1)$$

where l is the reaction path degeneracy, k_B is the Boltzmann constant, $Q_{\ddagger}$ and Q_R are partition functions for the TS and reactant, respectively, and E_0 is the zero-point barrier for the

TABLE 3: Comparison of the Rate Parameters for the Unimolecular Elimination of HCl from 1,2-Dichloroethane and Ethyl Chloride

Level of the theory/ Basis Set	log A		E_a[a]	
	$C_2H_4Cl_2 \rightarrow C_2H_3Cl + HCl$	$C_2H_5Cl \rightarrow C_2H_4 + HCl$	$C_2H_4Cl_2 \rightarrow C_2H_3Cl + HCl$	$C_2H_5Cl \rightarrow C_2H_4 + HCl$
HF/6-311^{2+}G**	14.95 ± 0.01	14.65 ± 0.01	69.45 ± 0.01	62.56 ± 0.01
with internal rotation	14.00 ± 0.01	13.95 ± 0.01	69.82 ± 0.01	62.18 ± 0.01
MP2(FULL)/6-31++G**	14.98 ± 0.01	14.60 ± 0.01	69.95 ± 0.02	66.30 ± 0.02
with internal rotation	14.00 ± 0.01	13.90 ± 0.01	70.25 ± 0.02	65.92 ± 0.02
B3LYP/6-311^{2+}G**	14.93 ± 0.01	14.63 ± 0.01	57.57 ± 0.02	53.67 ± 0.02
with internal rotation	14.01 ± 0.01	13.96 ± 0.01	57.91 ± 0.0	53.29 ± 0.02
experimental	13.98 ± 0.80[b]	13.84 ± 0.20[c]	57.8 ± 2.0[b]	57.8 ± 1.0[c]

[a] The E_o values are 65.8, 66.4, 53.9, and 67.6, 67.8, 55.5 for the *gauche*- and *trans*-1,2-DCE and they are 59.9, 63.7, 51.1 for EC at HF, MP2, and DFT levels, respectively. The theoretical results given for 1,2-DCE are Boltzmann weighted averages for the gauche and trans forms. [b] This work. [c] Data taken from ref 38.

reaction. The thermodynamic formulation of TST is then used to estimate the E_a and A on the basis of theory.[48] The rate constant for a unimolecular reaction is given by

$$k = le\frac{k_B T}{h}\exp\left[\frac{\Delta S^{\neq}}{R}\right]\exp\left[-\frac{E_a}{RT}\right] \quad (2)$$

Here, $\Delta S^{\neq}$ is the entropy of activation calculated using the partition functions of reactant and the TS. The A and E_a were calculated between 1050 and 1175 K (at 25 K intervals) using the HF, MP2, and DFT results using the largest basis set used here, 6-311++G**, and average values for this temperature range were estimated by fitting to the Arrhenius expression. For the 1,2-DCE frequency calculation at this level could not be done and hence the MP2/6-31G** frequencies were used in the calculation with MP2/6-311++G** barriers. Moreover, the rate constant was estimated for both trans and gauche forms and the total rate constant was calculated as follows:[49]

$$k = w_t k_t + w_g k_g \quad (3)$$

Here, w_i's are the weight factors of each conformer estimated from the Boltzmann distribution and k_i's are the rate constants calculated as above. The results are included in Table 3 along with the experimental results. At HF and MP2 levels, the activation energies calculated are very different from the experimental values but the DFT results are in reasonable agreement with experiment. The preexponential factor calculated from theory depends on how the torsional mode in the reactant molecules is treated. Activation energies also differ for the two models to a smaller extent as the thermal contributions are different for the two models. Both these factors are discussed in detail below.

The activation energy increases when going from HF to MP2 level by 3.7 and 0.5 kcal mol^{-1} for EC and 1,2-DCE, respectively. Considering the fact that at the HF level the barrier is already overestimated by 12 and 5 kcal mol^{-1}, it seems that including correlation at the MP2 level worsens the results compared to HF. This feature was seen in the results of work by Kirtman and co-workers on EC.[25] Also, our earlier work on HF/HCl elimination from HNFCl[45] identified this trend for HCl elimination. For HF elimination, the MP2 results were better than HF, but for HCl elimination they were not. Higher level (MP4) calculations were needed to improve the results. However, we noted that including electron correlation using DFT method improved the barrier estimate significantly at much lower computational cost. Here again, we find that the DFT level calculations give much better agreement with the experimental results. The activation energy calculated for 1,2-DCE and EC are 57.9 and 53.3 kcal mol^{-1}, respectively. The result for 1,2-DCE is virtually identical to the experimental value while that of EC is 4.5 kcal mol^{-1} smaller.

At all levels of theory, the HCl elimination barrier for 1,2-DCE is larger than that of EC. The difference in barrier is about 4 kcal mol^{-1} for MP2 and DFT calculations but it is 7 kcal mol^{-1} at the HF level. Our experimental results indicate that the activation energy for 1,2-DCE and EC are identical within the experimental uncertainty (2 kcal mol^{-1}). This is in agreement with the estimates of Weissman and Benson, who predicted a 1.5 kcal mol^{-1} increase.[31] It is likely that the β-substitution of Cl in EC leads to a modest increase in barrier for HCl elimination. Considering these two cases, the 12 kcal mol^{-1} increase predicted for HCl elimination barrier[17] on β-F substitution in CH_3COCl at the MP2/6-31G* level appears dramatic. As noted above, MP2 calculations appear to give large errors for HCl elimination barriers. Direct experimental determination and higher level calculations of HCl elimination barriers from CH_3COCl and FCH_2COCl would be essential before any serious conclusions can be drawn and such studies are planned.

The preexponential (A) factors calculated at all levels of theory depend on how one treats the hindered rotation about the C−C bond in the reactant.[5,6] Table 3 shows that the results based on torsional model (124 and 280 cm^{-1} for 1,2-DCE and EC, respectively) differ from experimental results on two counts. First the absolute value of A is significantly larger for both EC and 1,2-DCE. Theory overestimates A by a factor of 9.3 and 6.5 for 1,2-DCE and EC, respectively. Second, the ratio of the A factors for the two molecules are different. Experimental results show a 40% increase from EC to 1,2-DCE whereas the theory at all levels predicts a factor of 2.0 increase. The increase predicted by theory is largely due to the reaction path degeneracy, l being 4 for 1,2-DCE and 2 for EC for the torsional model. To be precise about 1,2-DCE, the l for the trans form is 4 and that for the gauche form is 2. However, there are two conformers with gauche geometry and using l as 4 for gauche takes care of this factor of 2 as well.

The complete torsional potential for 1,2-DCE has been calculated ab initio at MP4(SDQ) level of theory by Youssoufi et al.[44] They report a maximum barrier of 9 kcal mol^{-1} when both Cl atoms eclipse each other compared to the trans minimum shown in Figure 6. The energy difference between gauche and trans is only about 1.5 kcal mol^{-1} and the barrier for trans → gauche conversion is 5 kcal mol^{-1}. The barrier for rotation about C−C bond in EC[5] is smaller at 3.5 kcal mol^{-1}. We consider the extreme case of free internal rotation about the C−C bond at temperatures above 1000 K to see if it could account for the differences in the preexponential factor between EC and 1,2-DCE. The moments of inertia for the internal rotation are 35 and 3.0 amu Å^2 for 1,2-DCE and EC, respectively.[5] The

preexponential factors were calculated by using the partition function for internal rotation[48] instead of the torsional motion. In the free rotor model, the reaction path degeneracy for EC is 3 and that for 1,2-DCE is still 4. Within the temperature range of our study, using the free rotor model reduces the partition functions by a factor of 9 for 1,2-DCE and 5 for EC, compared to the torsional model. Thus, the *A* factors calculated by the free rotor model are in excellent agreement with the experiment. Accurate treatment of the torsional mode as a hindered rotor may increase the preexponential factor, but it is clear that the experimental and theoretical *A* factors would be in reasonable agreement. Thus, we conclude that even with longer C−Cl bond ("looser" TS), the experimental and theoretical preexponential factors could be reconciled with appropriate treatment of the torsional mode.

In our calculations, the frequencies have not been scaled as it was found not to have a serious effect on the preexponential factor during our work on CH_3COCl.[17] It is understandable given the fact that the rate depends on the ratio of partition functions for the TS and reactant. Moreover, scaling is useful for high-frequency stretching modes and when one considers the H/D isotopic effect. There are three (two) modes (CCCl deformation) with less than 500 cm^{-1} for 1,2-DCE (EC) ground state and four (three) for the TS. There is no reliable scaling procedure for these low-frequency modes, which contribute significantly to the preexponential factor. Moreover, harmonic approximation is certainly not valid in treating these low-frequency modes.

VI. Conclusions

The unimolecular HCl elimination from 1,2-DCE has been reported both experimentally and theoretically. A single pulse shock tube has been used for the experimental studies. Both ab initio and DFT methods have been employed to characterize the TS for HCl elimination from EC and 1,2-DCE. From the experimental results, the rate constant for the HCl elimination from 1,2-DCE is estimated to be $10^{13.98\pm0.80}$ exp $(-57.8 \pm 2.0/RT)$ s^{-1}. The activation energy for HCl elimination is nearly the same as that for EC.

The activation energies calculated for 1,2-DCE at HF, MP2, and DFT methods with the 6-311++G** basis set, differ from the experimental value by +12.0, +12.5, and 0.1 kcal mol^{-1}. The excellent agreement between DFT and experiment may be fortuitous as it underestimates the barrier for HCl elimination from EC by 4.5 kcal mol^{-1}. For EC also, HF and MP2 level calculations overestimate the barrier for HCl elimination by 4 and 8.5 kcal mol^{-1}, respectively. All three levels of theory predict the HCl elimination barrier to increase on β-Cl substitution of EC. The increase predicted by both MP2 and DFT calculations, which include electron correlation, is about 4 kcal mol^{-1}. This is in modest agreement with our experimental finding of no increase, given the 2 kcal mol^{-1} uncertainty in the experiments. The preexponential factors calculated using a free-rotor model for the torsional degree of freedom are in good agreement with experimental values.

Acknowledgment. We acknowledge the financial support from IISc-ISRO Space Technology Cell and the Director, Indian Institute of Science for establishing the high temperature chemical kinetics laboratory. E.A. thanks Prof. A. Lifshitz, Dr. G. O. Thomas, and Dr. J. V. Michael for helpful discussions in person, and Dr. W. Tsang for discussions through e-mail. Profs. D. W. Setser and K. L. Sebastian are acknowledged for stimulating discussions on TST. B.R. thanks Dr. R. B. Sunoj of The Ohio State University (U.S.A.) and Mr. K. R. Shamasundar of National Chemical Laboratory, (Pune, India) for fruitful discussions in running Gaussian 94 and Mr. Saravanan and Mr. Anandraj for help in the experiments. Mr. Nagaraja helped in running calculations on EC. L. Gangadharaih and Harikrishna are acknowledged for the workshop support in the establishment of the shock tube facility.

Supporting Information Available: Ten tables containing the optimized structures of *gauche*- and *trans*-1,2-DCE, EC, and TS for HCl elimination from both molecules and normal mode vibrational frequencies of all the five ground and transition state species. Results are included for HF, MP2(Full), and DFT(B3LYP) calculations with 6-31G*, 6-31G**, and 6-311++G** basis sets. This material is available free of charge via the Internet at http://pubs.acs.org.

References and Notes

(1) Barton, D. H. R.; Howlett, K. E. *J. Chem. Soc.* **1949**, 155 and 165.
(2) Howlett, K. E. *Discuss. Faraday Soc.* **1952**, *48*, 25.
(3) Holbrook, K. A.; Walker, R. W.; Watson, W. R. *J. Chem. Soc. B* **1971**, 577.
(4) Huybrechts, G.; Katihabwas, J.; Martens, G. J.; Nejszaten, M.; Olbregts, J. *Bull. Chem. Soc. Chim. Belg.* **1972**, *81*, 65.
(5) (a) Hassler, J. C.; Setser, D. W.; Johnson, R. L. *J. Chem. Phys.* **1966**, *45*, 3231; (b) Hassler, J. C.; Setser, D. W. *J. Chem. Phys.* **1966**, *45*, 3246.
(6) Dees, K.; Setser, D. W. *J. Chem. Phys.* **1968**, *49*, 1193.
(7) Roussel, P. B.; Lightfoot, P. D.; Carlap, F.; Catoire, V.; Lesclaux, R.; Forst, W. *J. Chem. Soc., Faraday Trans.* **1991**, *87*, 2367.
(8) Dyer, P. E.; Mathews, M.; Holbrook, K. A.; Oldershaw, G. A. *J. Chem. Soc., Faraday Trans.* **1991**, *87*, 2151.
(9) Ma, P.; Liu, J.; Chen, G.; Chu, M.; Jing, Y.; Wu, B. *J. Chem. Soc., Faraday Trans.* **1993**, *89*, 4171.
(10) Ashmore, P. G.; Owen, A. J. *J. Chem. Soc., Faraday Trans. 1* **1982**, *78*, 677.
(11) Incavo, J. A. *Ind. Eng. Chem. Res.* **1996**, *35*, 931.
(12) Borsa, A. G.; Herring, A. M.; McKinnon, J. T.; McCormick, R. L.; Yamamoto, S.; Teraoka, Y.; Natori, Y. *Ind. Eng. Chem. Res.* **1999**, *38*, 4259.
(13) Tsang, W.; Lifshitz, A. In *Handbook of Shock Waves, Vol. 3. Chemical Reactions in Shock Waves and Detonations;* Ben-Dor, G., Igra, O., Elperin, T., Lifshitz, A., Eds.; Academic Press: San Diego, 2001; and references therein.
(14) Clough, P. N.; Polanyi, J. C.; Taguchi, R. T. *Can. J. Chem.* **1970**, *48*, 2919.
(15) Sudbo, Aa. S.; Schulz, P. A.; Shen, Y. R.; Lee, Y. T. *J. Chem. Phys.* **1978**, 69, 2312.
(16) Quick, C. R.; Wittig, C. *J. Chem. Phys.* **1980**, *72*, 1694.
(17) Srivatsa, A.; Arunan, E.; Manke, G., II; Setser, D. W.; Sumathi, R. *J. Phys. Chem.* **1998**, *102*, 6412.
(18) Seakins, P. W.; Woodbridge, E. L.; Leone, S. R. *J. Phys. Chem.* **1993**, *97*, 5633.
(19) Tsang, W. *J. Chem. Phys.* **1964**, *41*, 2487.
(20) Milward, G. E.; Tschuikow-Roux, E. *Int. J. Chem. Kinet.* **1972**, *4*, 559.
(21) Cadman, P.; Day, M.; Kirk, A. W.; Trotman-Dickenson, A. F. *Chem. Commun.* **1970**, 203.
(22) Kato, S.; Morokuma, K. *J. Chem. Phys.* **1980**, *73*, 3900.
(23) Benito, R. M.; Santamaria, J. *J. Phys. Chem.* **1988**, *92*, 5028.
(24) Raff, L. M.; Graham, R. W. *J. Phys. Chem.* **1988**, *92*, 5111.
(25) Toto, J. L.; Pritchard, G. O.; Kirtman, B. *J. Phys. Chem.* **1994**, *98*, 8359, and references therein.
(26) (a) Rakestraw, D. J.; Holmes, B. E. *J. Phys. Chem.* **1991**, *95*, 3968. (b) Jones, Y.; Duke, D. W.; Tipton, D. L.; Holmes, B. E. *J. Phys. Chem.* **1990**, *94*, 4957.
(27) Chuchani, G.; Martin, I.; Rotinov, A.; Hernández, J. A.; Reikonnen, N. *J. Phys. Chem.* **1984**, *88*, 1563.
(28) Ho, W. P.; Barat, R. B.; Bozzelli, J. W. *Combust. Flame* **1992**, *88*, 265.
(29) Seetula, J. A. *J. Chem. Soc., Faraday Trans.* **1998**, *94*, 1933.
(30) Cardy, H.; Larrieu. C.; Chaillet, M.; Ollivier, J. *Chem. Phys.* **1993**, *169*, 305.
(31) Weissman, M.; Benson, S. W. *Int. J. Chem. Kinet.* **1984**, *16*, 307.
(32) Reddy, N. M.; Jagadish, G.; Nagashetty, K.; Reddy, K. P. J. *Sadhana-Proc. Ind. Acad. Sci.* **1996**, 741.

(33) Jagadish, G.; Reddy, N. M.; Reddy, K. P. J. *J. Spacecraft Rockets* **2000**, *37*, 137.

(34) Lifshitz, A.; Bauer, S. H.; Resler, E. L., Jr. *J. Chem. Phys.* **1963**, *38*, 2056.

(35) Cadman, P.; Thomas, G. O.; Butler, P. *Phys. Chem. Chem. Phys.* **2000**, *2*, 5411.

(36) (a) Tschuikow-Roux, E.; Simmie, J. M.; Quiring, W. J. *Astonamica Acta* **1970**, *15*, 511; (b) Tschuikow-Roux, E. *Phys. Fluids* **1965**, *8*, 821.

(37) Thomas, G. O. Fortran program rcmblast.for for simulation of shock and detonation waves. Implementation based on Gottlieb, J. J. *Comput. Phys.* **1988**, *78*, 160.

(38) Evans, P. J.; Ichimura, T.; Tschuikow-Roux, E. *Int. J. Chem. Kinet.* **1978**, *10*, 855.

(39) Tranter, R. S.; Sivaramakrishnan, R.; Srinivasan, N.; Brezinsky, K. *Int. J. Chem. Kinet.* **2001**, *33*, 722.

(40) Frisch, M. J.; Trucks, G. W.; Schlegel, H. B.; Gill, P. M. W.; Johnson, B. G.; Robb, M. A.; Cheeseman, J. R.; Keith, T.; Petersson, G. A.; Montgomery, J. A.; Raghavachari, K.; Al-Laham, M. A.; Zakrzewski, V. G.; Ortiz, J. V.; Foresman, J. B.; Cioslowski, J.; Stefanov, B. B.; Nanayakkara, A.; Challacombe, M.; Peng, C. Y.; Ayala, P. Y.; Chen, W.; Wong, M. W.; Andres, J. L.; Replogle, E. S.; Gomperts, R.; Martin, R. L.; Fox, D. J.; Binkley, J. S.; Defrees, D. J.; Baker, J.; Stewart, J. P.; Head-Gordon, M.; Gonzalez, C.; Pople, J. A. *Gaussian 94, Revision C.2;* Gaussian, Inc.: Pittsburgh, PA, 1995.

(41) Cadman, P.; Engelbrecht, W. J. *Chem. Commun*. **1970**, 453.

(42) Karra, S. B.; Senkan, S. M. *Ind. Eng. Chem. Res.* **1988**, *27*, 447.

(43) Kuramshina, G. M.; Weinhold, F.; Pentin, Y. A. *J. Chem. Phys.* **1998**, *109*, 7286.

(44) Youssoufi, Y. E.; Herman, M.; Lievin, J. *Mol. Phys.* **1998**, *94*, 461, and references therein.

(45) Shamasundar, K. R.; Arunan, E. *J. Phys. Chem. A* **2001**, *105*, 8533.

(46) *Tables of Molecular Vibrational Frequencies Consolidated*; Shimanouchi, T., Ed.; National Standard Reference Data Series, National Bureau of Standards: Washington, DC, 1972; Vol. 34, pp 97, 98.

(47) Schaftenaar, G.; Noordik, J. H. *Molden:* A pre- and postprocessing program for molecular and electronic structures. *J. Comput.-Aided Mol. Des.* **2000**, *14*, 123.

(48) Wright, M. R. *Fundamental Chemical Kinetics: An exploratory introduction to the concepts;* Harwood Publishing: Chichester, 1999.

(49) Chandra, A. K.; Uchimaru, T. *J. Phys. Chem. A* **1999**, *103*, 10874.